JOURNAL OF VIROLOGY, May 2011, p. 4184–4197 Vol. 85, No. 9
0022-538X/11/$12.00 doi:10.1128/JVI.02290-10

The Role of LAT in Increased CD8$^+$ T Cell Exhaustion in Trigeminal Ganglia of Mice Latently Infected with Herpes Simplex Virus 1$^\nabla$

Sariah J. Allen,[1] Pedram Hamrah,[2] David Gate,[3] Kevin R. Mott,[1] Dimosthenis Mantopoulos,[2] Lixin Zheng,[2] Terrence Town,[3] Clinton Jones,[4] Ulrich H. von Andrian,[5] Gordon J. Freeman,[6] Arlene H. Sharpe,[7] Lbachir BenMohamed,[8] Rafi Ahmed,[9] Steven L. Wechsler,[10,11,8] and Homayon Ghiasi[1]*

Center for Neurobiology and Vaccine Development, Ophthalmology Research, Department of Surgery, Cedars-Sinai Burns and Allen Research Institute, 8700 Beverly Boulevard, Los Angeles, California[1]; Massachusetts Eye and Ear Infirmary, Department of Ophthalmology, Harvard Medical School, Boston, Massachusetts[2]; Departments of Neurosurgery and Biomedical Sciences, Maxine Dunitz Neurosurgical Institute, Cedars-Sinai Medical Center, Los Angeles, California[3]; Department of Veterinary and Biomedical Sciences, Nebraska Center for Virology, University of Nebraska, Lincoln, Nebraska[4]; Department of Pathology, Harvard Medical School, Boston, Massachusetts[5]; Department of Medical Oncology, Dana-Farber Cancer Institute, Department of Medicine, Harvard Medical School, Boston, Massachusetts[6]; Department of Pathology, Harvard Medical School and Brigham and Women's Hospital, Boston, Massachusetts[7]; The Gavin Herbert Eye Institute and the Department of Ophthalmology, University of California, Irvine, School of Medicine, Irvine, California[8]; Emory Vaccine Center and Department of Microbiology and Immunology, Emory University School of Medicine, Atlanta, Georgia 30322[9]; Department of Microbiology and Molecular Genetics, University of California, Irvine, School of Medicine, Irvine, California[10]; and The Center for Virus Research, University of California, Irvine, Irvine, California[11]

Received 2 November 2010/Accepted 1 February 2011

Herpes simplex virus (HSV) infection is a classic example of latent viral infection in humans and experimental animal models. The HSV-1 latency-associated transcript (LAT) plays a major role in the HSV-1 latency reactivation cycle and thus in recurrent disease. Whether the presence of LAT leads to generation of dysfunctional T cell responses in the trigeminal ganglia (TG) of latently infected mice is not known. To address this issue, we used LAT-positive [LAT(+)] and LAT-deficient [LAT(−)] viruses to evaluate the effect of LAT on CD8 T cell exhaustion in TG of latently infected mice. The amount of latency as determined by quantitative reverse transcription-PCR (qRT-PCR) of viral DNA in total TG extracts was 3-fold higher with LAT(+) than with LAT(−) virus. LAT expression and increased latency correlated with increased mRNA levels of CD8, PD-1, and Tim-3. PD-1 is both a marker for exhaustion and a primary factor leading to exhaustion, and Tim-3 can also contribute to exhaustion. These results suggested that LAT(+) TG contain both more CD8$^+$ T cells and more CD8$^+$ T cells expressing the exhaustion markers PD-1 and Tim-3. This was confirmed by flow cytometry analyses of expression of CD3/CD8/PD-1/Tim-3, HSV-1, CD8$^+$ T cell pentamer (specific for a peptide derived from residues 498 to 505 of glycoprotein B [gB$_{498–505}$]), interleukin-2 (IL-2), and tumor necrosis factor alpha (TNF-α). The functional significance of PD-1 and its ligands in HSV-1 latency was demonstrated by the significantly reduced amount of HSV-1 latency in PD-1- and PD-L1-deficient mice. Together, these results may suggest that both PD-1 and Tim-3 are mediators of CD8$^+$ T cell exhaustion and latency in HSV-1 infection.

One of the hallmarks of herpes simplex virus (HSV) infection is the ability of the virus to establish latency in sensory neurons of an infected host (19, 71, 76). Once acquired, latent infections demonstrate a lifelong pattern of episodic recurrence, such that infected individuals serve as permanent carriers who are intermittently infectious (24, 36, 70). At various times throughout the life of the latently infected individual, the virus may reactivate, travel back to the original site of infection, and cause recurrent disease (6, 80). In neurons, expression of the more than 80 genes of HSV-1 that occurs during lytic infection is drastically modified. The latency-associated transcript (LAT) is the only gene product consistently detected in abundance during latency in infected mice, rabbits, and humans (26, 63, 71, 76, 77).

The LAT gene is located in the long repeats of the virus and is, therefore, present in two copies per genome (43). The primary LAT transcript is 8.3 kb and is unstable. A very stable 2-kb LAT, which is also referred to as the "stable" or "major" LAT (75–77), is derived from the primary transcript by splicing (14). The 2-kb LAT accumulates in the nucleus of latently infected neurons but can also be detected in the cytoplasm (2, 52, 76, 77). A second LAT RNA of 1.3 to 1.5 kb (63), which is apparently derived from the 2-kb LAT by splicing (12, 18), is also abundant during latency.

There is a general belief that the HSV-1 genome is maintained in a quiescent state in sensory neurons during latency. This state is characterized by the absence of detectable viral protein synthesis. However, studies in mice indicate that lytic transcripts and proteins may be expressed at very low levels in latently infected ganglia (15, 40). There is also human observational data based on tissue sampling which demonstrated

* Corresponding author. Mailing address: Center for Neurobiology and Vaccine Development, D2024, Cedars-Sinai Burns and Allen Research Institute, 8700 Beverly Blvd., Los Angeles, CA 90048. Phone: (310) 423-0593. Fax: (310) 423-0302. E-mail: ghiasih@cshs.org.
$^\nabla$ Published ahead of print on 9 February 2011.

expression of HSV-1 genes during latency (11, 28, 61, 62). Whether this low-level HSV-1 gene expression represents reactivation events or indicates continued low-level viral gene expression during latency remains unclear. LAT is important for the high, wild-type (wt) rate of *in vivo* spontaneous (55) and induced (26) reactivation from latency. LAT has antiapoptosis activity (7, 8, 29, 31, 54, 56). Replacing LAT with different alternative antiapoptosis genes restores the wild-type reactivation phenotype to a LAT-deficient [LAT(−)] virus (32, 57) indicating that LAT's antiapoptosis activity is critical for how LAT enhances the reactivation phenotype.

Recently, work on T cell exhaustion confirmed that the antigenic load during chronic lymphocytic choriomeningitis virus (LCMV) infection of mice directly contributes to $CD8^+$ T cell exhaustion (50). Exhausted T cells have significantly reduced function and proliferation (5, 10). Exhaustion is a T cell response to continued long-term exposure to the antigen (Ag) specific to the T cell (50). PD-1 (programmed death cell receptor 1) is a receptor protein inducibly expressed on T cells (37). Binding of the PD-1 ligands (PD-L1 and PD-L2) to PD-1 results in downregulation of T cell functions and exhaustion (37). Thus, PD-1 is both a marker and a mediator of exhaustion (5). Similarly, Tim-3 (T cell immunoglobulin and mucin domain-containing protein 3) upregulation has also been correlated with T cell exhaustion (23, 30, 33). Previously, we found that mice latently infected with wild-type HSV-1 have increased LAT RNA, more CD8 mRNA, and more PD-1 mRNA in their trigeminal ganglia (TG) (45). This suggested that TG harboring higher levels of HSV-1 latency had more exhausted CD8 T cells. However, definitive evidence for this conclusion requires analysis of CD8 T cells rather than measurements of CD8 and PD-1 mRNA levels in total TG extracts. In addition, the potential role of LAT in T cell exhaustion is unclear. More LAT may result in more reactivation and higher antigen loads, resulting in more CD8 T cell exhaustion. Alternatively, LAT could cause CD8 T cell exhaustion by some other means, and the CD8 T cell exhaustion could result in more latency. To address these issues, we examined CD8 T cell exhaustion in TG of mice latently infected with LAT-positive [LAT(+)] versus LAT(−) viruses and also determined if HSV-1 latency levels were altered in PD-1-, PD-L1-, and PD-L2-deficient mice. Here, we report significantly increased numbers of PD-1- and Tim-3-positive CD8 T cells (i.e., exhausted CD8 T cells) in TG of mice latently infected with LAT(+) versus LAT(−) virus and significantly decreased HSV-1 latency in PD-$1^{-/-}$ and PD-$L1^{-/-}$ mice compared to wt or PD-$L2^{-/-}$ mice. Thus, these studies point to key rolls for PD-1 and Tim-3 in controlling HSV latency.

MATERIALS AND METHODS

Virus and mice. Plaque-purified HSV-1 strains McKrae (wild type; LAT positive) and dLAT2903 (LAT deficient; see below) were grown in rabbit skin (RS) cell monolayers in minimal essential medium (MEM) containing 5% fetal calf serum (FCS), as described previously (53, 55). In this study mice were ocularly infected with wt HSV-1 strain McKrae [LAT(+)] or three different LAT-deficient viruses: (i) dLAT2903 in which both copies of the LAT promoter (one in each viral long repeat) and the first 1,667 nucleotides (nt) of the LAT transcript are deleted [LAT(−)A] (55); (ii) HSV-gK^3 (47) in which LAT nt 76 to 1499 in both copies of LAT are replaced by the open reading frame (ORF) encoding HSV-1 glycoprotein K (resulting in the virus containing three copies of gK) [LAT(−)B] (47); and (iii) HSV-CD80 (unpublished data), containing the CD80 ORF in place of LAT nt 76 to 1499 in both copies of LAT [LAT(−)C].

Wild-type C57BL/6 and BALB/c mice were purchased from Jackson Laboratories. C57BL/6 PD-$1^{-/-}$, C57BL/6 PD-$L1^{-/-}$, BALB/c PD-$L1^{-/-}$, and BALB/c PD-$L2^{-/-}$ mice have been reported previously (38, 41) and were bred in-house. There were no differences in terms of survival rates or levels of eye disease between infected wild-type BALB/c or wild-type C56BL/6 mice compared to infected C57BL/6 PD-$1^{-/-}$, C57BL/6 PD-$L1^{-/-}$, BALB/c PD-$L1^{-/-}$, and BALB/c PD-$L2^{-/-}$ mice. All animal procedures adhered to the Association for Research in Vision and Ophthalmology (ARVO) statement for the Use of Animals in Ophthalmic and Vision Research and according to institutional animal care and use guidelines.

Ocular infection. Mice with a C57BL/6 background were infected ocularly with 2×10^5 PFU of each virus while mice with a BALB/c background were infected ocularly with 2×10^4 PFU of HSV-1 in order to increase survival. Each virus was suspended in 2 μl of tissue culture medium and administered as an eye drop without prior corneal scarification.

Preparation of TG for immunostaining. The trigeminal ganglia (TG) of naive and infected mice were removed at necropsy approximately 30 days postinfection (p.i.), embedded in optimal cutting temperature compound ([OCT] Tissue-Tek; Sakura) for cryosectioning, and stored at −80°C. Transverse sections were cut 15 μm thick and air dried for 15 min. Representative sections (spaced 50 μm apart) throughout the TG were incubated for 30 min in Dako Serum Free Protein Block. Rat anti-mouse CD8a (clone 53-6.7; eBioscience, San Diego, CA), goat anti-mouse Tim-3 (R&D Systems, Minneapolis, MN), and Armenian hamster anti-PD-1 (clone J43; eBioscience) antibodies were incubated in protein block at 4°C overnight. After three rinses for 5 min each in phosphate-buffered saline (PBS), slides were incubated for 1 h at 25°C with secondary antibody labeled with Alexa Fluor-488 (green), -594 (red), or -647 (magenta) (Invitrogen, Carlsbad, CA). Sections were washed three times with PBS, air dried, and mounted with Prolong Gold 4′,6′-diamidino-2-phenylindole (DAPI) mounting medium (Invitrogen). The fluorophores were imaged in separate channels with a Zeiss Apo-Tome-equipped Axio Imager Z1 (Carl Zeiss Microimaging). Images were then analyzed using ImageJ software, release 1.40g. The number of cells immunopositive for each antibody was counted in a double-blind fashion from the entire tissue section. To reduce possible staining or sampling variability, three consecutive sections from each tissue were examined on each slide. One section was used to quantitate the number and distribution of cells. The second and third sections were used to verify these results, thereby confirming accuracy and ensuring a lack of artifacts due to staining or tissue manipulation.

Cell surface and intracellular cytokine staining of isolated cells from latently infected TG. TG from five naive or infected animals per group were harvested and pooled together for processing after day 30 p.i. TG were digested in a PBS solution containing collagenase type I (3 mg/ml; Sigma-Aldrich, St. Louis, MO) and incubated for 2 h at 37°C, with trituration approximately every 30 min, as we described previously (48). Single-cell suspensions were washed with PBS, and T cells were isolated using magnetic labeling and separation columns (Pan T Cell Isolation Kit, catalog number 130-095-130; Miltenyi Biotec Inc., Auburn, CA) as per the manufacturer's protocol. Briefly, non-T cells (i.e., B, NK, dendritic, macrophage, and erythroid cells) were indirectly magnetically labeled with a cocktail of biotin-conjugated antibodies and antibiotin microbeads. T cells were subsequently isolated by depletion of the magnetically labeled non-T cells onto a column in a magnetic field. The recovered cells were washed, divided by half, stained with monoclonal antibodies (MAbs), and subjected to standard multicolor fluorescence-activated cell sorter (FACS) analysis to assess both surface and intracellular expression of various markers. In some studies we used Pacific Blue anti-mouse CD8α, allophycocyanin (APC)-conjugated anti-mouse Tim-3, fluorescein isothiocyanate (FITC)-conjugated anti-mouse PD-1, peridinin chlorophyll protein (PerCP)-conjugated anti-mouse CD4, and phycoerythrin (PE)-conjugated HSV-1 $CD8^+$ T cell pentamer specific for a peptide derived from residues 498 to 505 of gB ($gB_{498\text{-}505}$). In other studies we used Pacific Blue anti-mouse CD8α, APC-conjugated anti-mouse Tim-3, FITC-conjugated anti-mouse PD-1, PerCP-conjugated anti-mouse CD4, and PE-conjugated HSV-1 $gB_{498\text{-}505}$-specific $CD8^+$ T cell pentamer. In the second set of the study we used APC-conjugated anti-mouse CD8α, PerCP-conjugated anti-mouse CD4, FITC-conjugated anti-mouse tumor necrosis factor alpha (TNF-α), PE-Cy7-conjugated anti-mouse gamma interferon (IFN-γ), and Pacific Blue-conjugated anti-mouse interleukin-2 (IL-2). (All antibodies were from eBioscience and BD Biosciences, San Diego, CA, and HSV-1 $gB_{498\text{-}505}$ pentamer was from ProImmune Inc., Bradenton, FL.) GolgiStop reagent (containing monensin) and all reagents for cell fixation and permeabilization (BD Cytofix/Cytoperm Plus; BD Biosciences, San Diego, CA) were used following the manufacturer's protocol. For cell surface staining, isolated T cells were incubated with CD4/CD8/PD-1/Tim-3/$gB_{498\text{-}505}$

TABLE 1. Level of $CD8^+$ T cell exhaustion in TG of latently infected mice[a]

Virus	% $CD8^+$ T cells positive for the indicated exhaustion marker in:					
	gB^+ population			gB^- population		
	$PD\text{-}1^+$	$Tim\text{-}3^+$	$PD\text{-}1^+$ $Tim3^+$	$PD\text{-}1^+$	$Tim\text{-}3^+$	$PD\text{-}1^+$ $Tim3^+$
LAT(+)	7.4 ± 1.7	51.4 ± 13	1.1 ± 0.2	18.5 ± 6	2 ± 1	1.9 ± 0.3
LAT(−)A	7.7 ± 2.3	50 ± 8	1.5 ± 0.7	17.8 ± 8	1 ± 0.2	0.5 ± 0.2
P value	0.9	0.9	0.6	0.9	0.4	0.2

[a] C57BL/6 mice were ocularly infected with LAT(+) or LAT(−)A virus. At 30 days p.i., TG from five mice per group were harvested, pooled, and digested with collagenase (400 IU/TG). The cell suspension was filtered through a 45-mm-pore-size cell strainer and then filtered through a magnetic cell sorting T cell isolation column; cells were stained with Pacific Blue-anti-CD8, APC-anti-Tim-3, FITC-anti-PD-1, and PE-gB-pentamer and analyzed by FACS. Average percentages of $CD8^+$ $PD\text{-}1^+$, $CD8^+$ $Tim\text{-}3^+$, and $CD8^+$ $PD\text{-}1^+$ $Tim\text{-}3^+$ T cells are shown. The experiment was repeated four times for a total of 40 TG (20 mice/group). Values are means ± standard error of the means.

MAbs following the manufacturer's protocol. For intracellular staining, single-cell suspensions of T cells from naive, LAT(+) and LAT(−)A virus-infected mice were incubated at 37°C and 5% CO_2 for 4 h in the presence of BD GolgiStop. At the end of the incubation, cells were washed and resuspended in FACS buffer and incubated for 15 min at 4°C with purified 2.4G2 antibody (Fc block, catalog number 553142; BD Biosciences) followed by subsequent incubation with CD4 and CD8 MAbs at 4°C for 30 min. Stained cells were washed twice with FACS buffer and fixed with 250 μl of BD Cytofix/Cytoperm solution for 20 min at 4°C. Following fixation, the cells were washed twice in BD Biosciences Perm/Wash buffer and resuspended in the same buffer for intracellular cytokine staining with IL-2, IFN-γ, and TNF-α. The cells were washed again and analyzed using multicolor five-laser FACScan instrumentation (Becton Dickinson). In some of the analyses, due to the limited number of cells in each quadrant and the high number of experimental groups, we presented the FACS analyses for exhaustion markers (Table 1) and cytokine production (Table 2) as tables instead of scatter plots. Experiments were repeated four times.

Microscopy for HSV-1. The TG sections from mice latently infected with LAT(+) and LAT(−)A viruses were incubated for 30 min in Dako serum-free protein block. MAP-2 (microtubule associated protein 2) (AB5622; Millipore) antibody was incubated overnight at 4°C at 1:1,000 dilution in Dako protein block. Sections were washed, incubated for 1 h at room temperature with FITC-conjugated HSV-1 (specific for gC) (catalog number 20-902-170310; GenWay) antibody and anti-rabbit Alexa Fluor-647 secondary antibody in Dako protein block at a 1:100 dilution of each antibody. Sections were washed three times with PBS, air dried, and mounted with Prolong Gold DAPI mounting medium (Invitrogen). Images were captured at magnifications of ×20 and ×63 in independent fluorescence channels using a Nikon C1 eclipse inverted confocal microscope.

DNA extraction and PCR analysis for HSV-1 genomic DNA. DNA was isolated from homogenized individual TG using the commercially available DNeasy Blood and Tissue Kit (catalog number 69506; Qiagen, Stanford, CA) according to the manufacturer's instructions. PCR analyses were done using gB-specific primers (forward, 5′-AACGCGACGCACATCAAG-3′; reverse, 5′-CTGGTAC GCGATCAGAAAGC-3′; and probe, 5′-FAM-CAGCCGCAGTACTACC-3′, where FAM is 6-carboxyfluorescein). The amplicon length for this primer set is 72 bp. Relative copy numbers for gB DNA was calculated using standard curves generated from the plasmid pAc-gB1. In all experiments glyceraldehyde-3-phosphate dehydrogenase (GAPDH) was used for normalization of transcripts.

RNA extraction, cDNA synthesis, and TaqMan RT-PCR. Individual TG from naive mice and mice that survived ocular infection were collected approximately 30 days postinfection and immersed in RNAlater RNA stabilization reagent and stored at −80°C until processing. Tissue processing, total RNA extraction, and RNA yield were carried out as we have described previously (46, 47). Following RNA extraction, 1,000 ng of total RNA was reverse transcribed using random hexamer primers and murine leukemia virus (MuLV) reverse transcriptase from a High Capacity cDNA Reverse Transcription Kit (Applied Biosystems, Foster City, CA), in accordance with the manufacturer's recommendations. The levels of various RNAs were evaluated using commercially available TaqMan Gene Expression Assays (Applied Biosystems, Foster City, CA) with optimized primer and probe concentrations. Primer probe sets consisted of two unlabeled PCR primers and the FAM dye-labeled TaqMan MGB probe formulated into a single mixture. Additionally, all cellular amplicons included an intron-exon junction to eliminate signal from genomic DNA contamination. The ABI assays used in this study were as follows: (i) for CD4, assay Mm00442754_m1 (amplicon length, 72 bp); (ii) for CD8 (α chain), Mn01182108_m1 (67 bp); (iii) for CD8 (β chain), Mm_00438116_m1 (89 bp); (iv) for PD-1 (also known as CD279), Mm00435532_m1 (65 bp); (v) for Tim-3, Mm00454540_m1 (98 bp); (vi) for IL-21, Mm00517640_m1 (67 bp); (vii) for IL-2, Mm00434256_m1 (82 bp); (viii) for IFN-γ, Mm00801778_m1 (101 bp); and (ix) for TNF-α, Mm00443258_m1 (81 bp). The custom-made primers and probe set for LAT were as follows: forward primer, 5′-GGGTGGGCTCGTGTTACAG-3′; reverse primer, 5′-GGACGGG TAAGTAACAGAGTCTCTA-3′; and probe, 5′-FAM-ACACCAGCCCGTTC TTT-3′ (amplicon length of 81 bp, corresponding to LAT nt 119553 to 119634). Quantitative reverse transcription-PCR (qRT-PCR) was performed using an ABI Prism 7900HT Sequence Detection System (Applied Biosystems, Foster City, CA) in 384-well plates, as we described previously(46, 47). Real-time PCR was performed in triplicate for each tissue sample. The threshold cycle (C_T) value, which represents the PCR cycle at which there is a noticeable increase in the reporter fluorescence above baseline, was determined using SDS software, version 2.2. GAPDH RNA was used for normalization of transcripts.

Statistical analysis. Student's *t* test, analysis of variance (ANOVA), and chi-square tests were performed using the computer program Instat (GraphPad, San

TABLE 2. Number of T cells per TG and percentage of cytokine-producing T cells in TG of latently infected mice[a]

Virus	$CD8^+$ T cell population				$CD4^+$ T cell population			
	Avg no. of cells/TG	% Producing the indicated cytokine			Avg no. of cells/TG	% Producing the indicated cytokine		
		IL-2	TNF-α	IFN-γ		IL-2	TNF-α	IFN-γ
LAT(+)	377 ± 55	4 ± 2	3 ± 1	32 ± 13	11 ± 2	31 ± 24	30 ± 24	69 ± 22
LAT(−)A	173 ± 34	4 ± 1	2 ± 1	41 ± 4	27 ± 8	60 ± 18	42 ± 19	81 ± 8
P value	0.02	1.0	0.76	0.56	0.1	0.37	0.71	0.6

[a] C57BL/6 mice were ocularly infected with LAT(+) or LAT(−)A virus. At 30 days p.i., TG from five mice per group were harvested, pooled, and digested with collagenase (400 IU/TG). The cell suspension was filtered through a 45-mm-pore-size cell strainer and then filtered through a magnetic cell sorting T cell isolation column; cells were stained with APC-anti-CD8, PerCP-anti-CD4, Pacific Blue-anti-IL-2, FITC-anti-TNF-α, and PE-Cy7-labeled anti-IFNγ and analyzed by FACS. Average numbers of $CD4^+$ and $CD8^+$ T cells per TG as well as the percentages of cytokine-producing $CD8^+$ and $CD4^+$ T cells are shown. The experiment was repeated four times for a total of 40 TG (20 mice/group). Values are means ± standard error of the means.

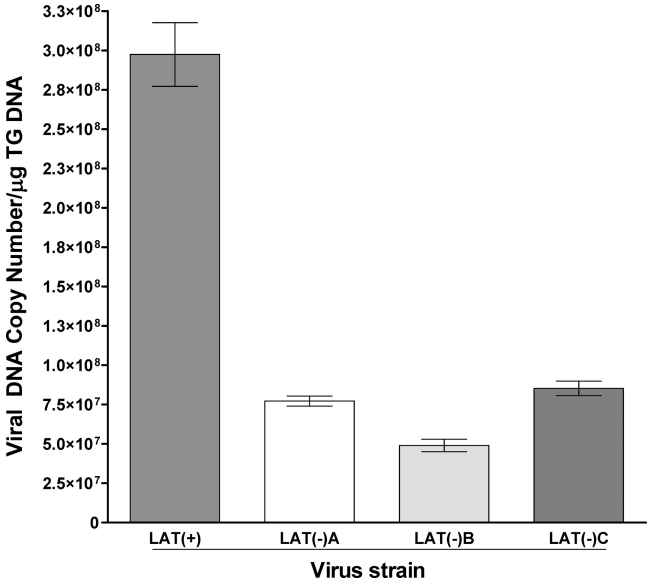

FIG. 1. Quantitation of viral DNA in TG of latently infected mice. C57BL/6 mice were ocularly infected with HSV-1 strain McKrae [LAT(+)[, dLAT2903 [LAT(−)A], HSV-gK^3 [LAT(−)B], which expresses two additional copies of gK in place of LAT, and HSV-CD80 [LAT(−)C], which expresses two copies of CD80 in place of LAT. On day 30 p.i., TG were harvested from the latently infected surviving mice. Quantitative PCR was performed on each individual mouse TG. In each experiment, an estimated relative copy number of the HSV-1 gB gene was calculated using standard curves generated from pGem-gB1. Briefly, DNA template was serially diluted 10-fold such that 5 μl contained from 10^3 to 10^{11} copies of gB DNA, and then the sample was subjected to TaqMan PCR with the same set of primers. By comparing the normalized threshold cycle of each sample to the threshold cycle of the standard, the copy number for each reaction was determined. GAPDH expression was used to normalize the relative expression of viral (gB) DNA in the TG. Each point represents the mean ± standard error of the mean from 56 TG for LAT(+) and LAT(−)A viruses and 20 TG each for LAT(−)B and LAT(−)C viruses.

Diego, CA). Results were considered statistically significant at a P value of <0.05.

RESULTS

Decreased viral DNA in TG of mice latently infected with LAT(−) versus LAT(+) virus. C57BL/6 mice were infected ocularly with 2×10^5 PFU/eye of wt [LAT(+)] HSV-1 strain McKrae, dLAT2903 [LAT(−)A], HSV-gK^3 [LAT(−)B], or HSV-CD80 [LAT(−)C] virus. Individual TG from surviving mice were isolated on day 30 postinfection (p.i.), and total DNA was isolated. TaqMan PCR was performed to quantitate viral DNA levels as described in Materials and Methods. Cellular GAPDH DNA was used as an internal control. The combined data from three separate experiments are shown in Fig. 1. The amounts of viral DNA during latency in mice infected with each of the three LAT(−) viruses were similar (Fig. 1) [for LAT(−)A, LAT(−)B, and LAT(−)C, $P > 0.05$). The mice latently infected with LAT(+) virus had at least 3-fold more viral DNA than any of the groups latently infected with LAT(−) virus (Fig. 1) ($P < 0.0001$, Student's t test). Thus, all three LAT(−) viruses appeared to have reduced HSV-1 latency based on total viral genome copies in TG extracts. These results are consistent with previously reported studies showing that LAT increased the amount of viral latency (58, 68, 69). These results suggest that a LAT function is required for efficient latency in TG of infected mice.

Increased number of CD8 T cells in TG of mice latently infected with LAT(+) versus LAT(−) virus. Mice were infected as above with LAT(+) or LAT(−)A virus. Half of the T cells isolated from TG of five mice were stained for CD8$^+$ T cell expression. Figure 2 shows a representative flow cytometric analysis of the number of total T cells that are CD8$^+$ in TG of mice latently infected with LAT(+) virus (Fig. 2A, middle panel) versus LAT(−)A virus (Fig. 2B, middle panel). Compared to TG from mice latently infected with LAT(−)A virus, TG from mice latently infected with LAT(+) virus contained a higher number of CD3$^+$ CD8$^+$ T cells (3,020 versus 786) (compare Fig. 2A and B). These results suggest that TG from mice latently infected with LAT(+) virus contained more CD3$^+$ CD8$^+$ T cells than TG from mice latently infected with LAT(−)A virus. This result is consistent with a previous study showing that more CD8$^+$ T cells were detected in the presence of LAT in latently infected mice (7).

Increased PD-1$^+$ and Tim-3$^+$ CD8 T cells in TG of mice latently infected with LAT(+) versus LAT(−) virus. To examine CD8 T cell exhaustion, the CD8 T cells discussed above were first gated for the presence of the T cell exhaustion markers PD-1 and Tim-3 (23, 30, 33). Figure 2 shows a representative flow cytometry analysis of the number of CD3$^+$ CD8$^+$ T cells in LAT(+) TG that are CD8$^+$ Tim-3$^+$ (Fig. 2A, left panel) and CD8$^+$ PD-1$^+$ (Fig. 2A, right panel) versus CD8$^+$ Tim-3$^+$ (Fig. 2B, left panel) and CD8$^+$ PD-1$^+$ (Fig. 2B, right panel) in LAT(−)A TG. We detected an increase in the number of CD8$^+$ Tim-3$^+$ T cells in LAT(+) TG compared to the number in LAT(−)A TG (974 versus 240, respectively) (compare Fig. 2A and B, left panels). We also detected an increase in the number of CD8$^+$ PD-1$^+$ T cells in LAT(+) TG compared to LAT(−)A TG (593 versus 217, respectively) (compare Fig. 2A and B, right panels). The flow cytometry results described in Fig. 2A and B represent the number of positive cells from five pooled TG, and the figure presented is the average of four independent experiments. Figure 2C shows the average number of CD8$^+$ PD-1$^+$ and CD8$^+$ Tim-3$^+$ T cells per individual TG. The TG from mice latently infected with LAT(+) virus had significantly more CD8$^+$ PD-1$^+$ T cells than TG from LAT(−)A virus-infected mice (Fig. 2C, left) ($P = 0.01$, Student's t test). Similarly, the TG from mice latently infected with LAT(+) virus also had a significantly higher number of CD8$^+$ Tim-3$^+$ T cells than TG from LAT(−)A virus-infected mice (Fig. 2C, right) ($P = 0.02$, Student's t test). These results suggest that both PD-1 and Tim-3 exhaustion markers are present on T cells in latently infected mice and that the effect is greater in the presence of LAT. This result is consistent with a recent study showing that both PD-1 and Tim-3 expression are contributing to T cell exhaustion during LCMV chronic viral infection (30).

Finally, to rule out the potential of T cell contamination from the lymphatic system, we performed FACS analysis on TG and spleen from naive mice (Fig. 2D shows a representative histogram and dot plot). Our results show that only one CD3$^+$ CD4$^+$ and five CD3$^+$ CD8$^+$ T cells were present in five TG while abundant numbers of CD3$^+$ CD4$^+$ and CD3$^+$ CD8$^+$

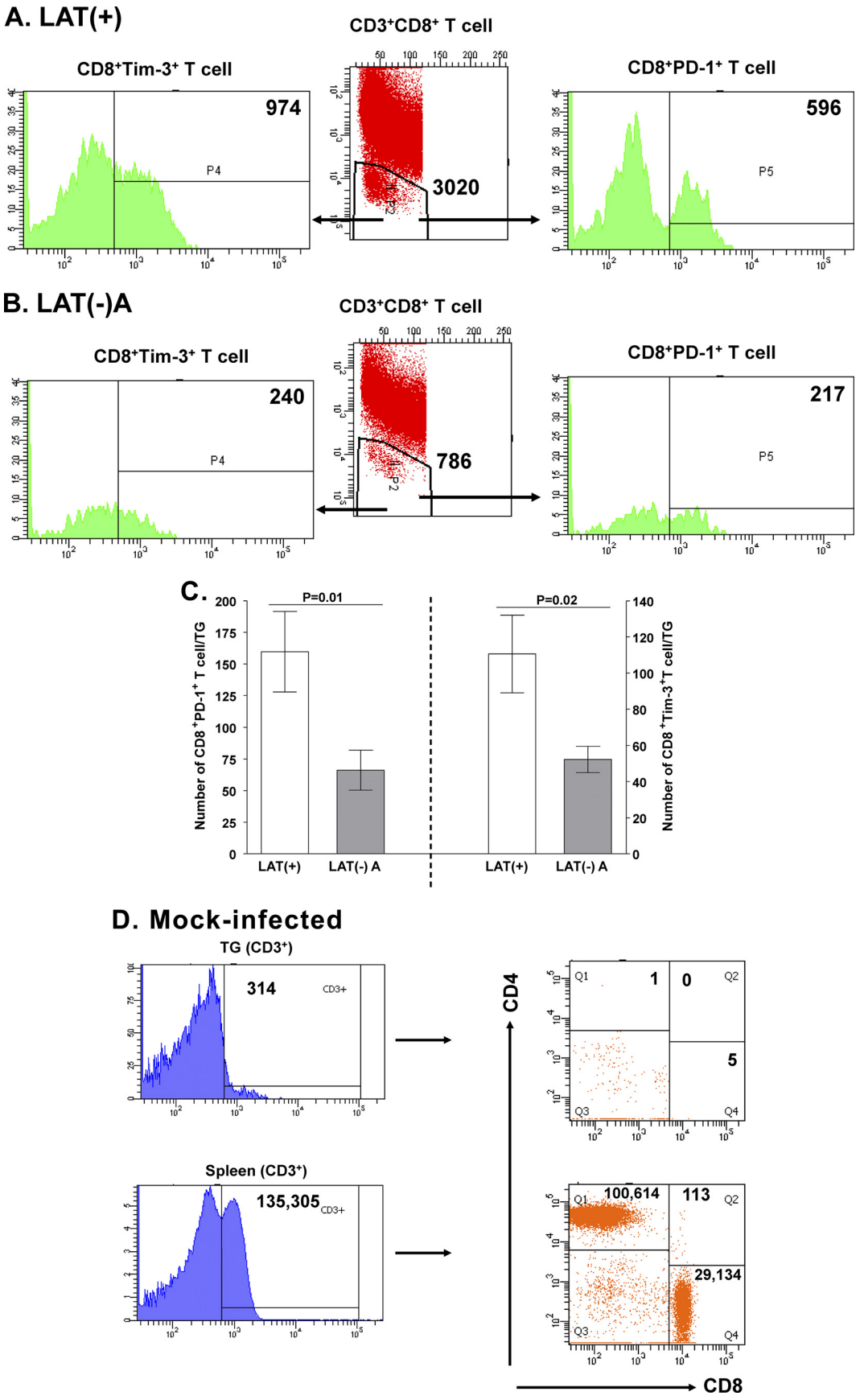
A. LAT(+)
CD3+CD8+ T cell
CD8+Tim-3+ T cell
974
P4
3020
CD8+PD-1+ T cell
596
P5
B. LAT(-)A
CD3+CD8+ T cell
CD8+Tim-3+ T cell
240
P4
786
CD8+PD-1+ T cell
217
P5
C.
P=0.01
P=0.02
Number of CD8+PD-1+ T cell/TG
Number of CD8+Tim-3+T cell/TG
LAT(+)
LAT(-) A
LAT(+)
LAT(-) A
D. Mock-infected
TG (CD3+)
314
CD3+
Spleen (CD3+)
135,305
CD3+
CD4
CD8
1
0
5
100,614
113
29,134

T cells were detected in the spleens of the same mice (Fig. 2D). These results suggest that presence of T cells in TG of latently infected mice is due to infection rather than lymphatic contamination.

To confirm the flow cytometry results described above (Fig. 2) that both PD-1 and Tim-3 are present on T cells from latently infected mice, sections of TG from naïve mice and mice latently infected with LAT(+) and LAT(−)A viruses were doubly stained with anti-CD8 and anti-PD-1 or with anti-CD8 and anti-Tim-3 antibodies, as described in Materials and Methods. Confocal microscopy showed a qualitative increase in the number of $CD8^+$ $PD\text{-}1^+$ (Fig. 3A) and $CD8^+$ $Tim\text{-}3^+$ (Fig. 3B) T cells in the TG of mice latently infected with LAT(+) virus compared to TG of mice infected with LAT(−)A virus. We did not observe any $CD8^+$ T cells in TG of naive mice. Quantitative image analyses of stained TG revealed a significant increase in $CD8^+$ $PD\text{-}1^+$ T cells in LAT(+) TG versus LAT(−)A TG (Fig. 3C, left) ($P < 0.001$, Student's *t* test). A similar increase in $CD8^+$ $Tim\text{-}3^+$ T cells in LAT(+) TG versus LAT(−)A TG was also detected (Fig. 3C, right) ($P < 0.001$, Student's *t* test). These results are consistent with the flow cytometry results described above (Fig. 2) and suggest that the number of CD8 T cells expressing the exhaustion markers PD-1 and Tim-3 was higher in TG of mice latently infected with LAT(+) virus than in those infected with LAT(−)A virus and suggest that both PD-1 and Tim-3 may be contributing to likely T cell exhaustion.

There are more HSV-1-specific gB^+ CD8 T cells in LAT(+) virus-infected TG. The above results demonstrated that more $CD3^+$ $CD8^+$ T cells are present in LAT(+) TG than in LAT(−)A TG and that these T cells displayed an increase in exhaustion markers. To determine whether these $CD8^+$ T cells are HSV-1 specific, TG from LAT(+) and LAT(−)A virus-infected mice were stained with $gB_{498–505}$-specific $CD8^+$ T cell pentamer as described in Materials and Methods. Figure 4 shows a representative flow cytometric analysis of the total population of $CD8^+$ T cells that are $gB_{498–505}$ pentamer positive or negative in TG of LAT(+) versus LAT(−)A TG from four independent experiments. We again observed an increase in the number of $CD8^+$ T cells in LAT(+) TG compared to LAT(−)A TG (2,894 versus 953 cells) (Fig. 4A and B, respectively), consistent with our earlier FACS (Fig. 2) and immunohistochemistry (IHC) (Fig. 3) results. There were also more $CD8^+$ gB^+ (HSV-1-specific) T cells in the LAT(+) TG than the LAT(−)A TG (1,243 versus 362) (compare Fig. 4A and B). The flow cytometry results described in Fig. 4A and B represent the number of positive cells from five pooled TG. The average numbers of gB^+ $CD8^+$ and gB^- $CD8^+$ T cells per individual TG from four separate experiments were quantified and are shown in Fig. 4C. Individual LAT(+) virus-infected TG contained a higher number of gB^+ $CD8^+$ T cells than the LAT(−)A virus-infected TG (Fig. 4C, left) ($P = 0.01$). Similarly LAT(+) virus-infected TG also contained a higher number of gB^- $CD8^+$ T cells than the LAT(−)A virus-infected TG (Fig. 4C, right) ($P = 0.002$). These results suggest (i) that higher specificity of $CD8^+$ T cells in LAT(+) TG does not contribute to better protection from latency and (ii) that less reactivation in LAT(−) TG produced less HSV-1 specificity of $CD8^+$ T cells.

Relationship of Tim-3 and PD-1 exhaustion markers in HSV-specific CD8 T cells. To confirm if the HSV specificity of T cells correlates with higher or lower levels of PD-1 and Tim-3 expression, T cells isolated from latently infected mouse TG were stained for CD8, $gB_{498–505}$ pentamer, PD-1, and Tim-3 as described in Materials and Methods. Table 1 shows the percentages of $CD8^+$ T cells that are PD-1 positive ($PD\text{-}1^+$), $Tim\text{-}3^+$, or $PD\text{-}1^+$ $Tim\text{-}3^+$ in both gB^+ and gB^- populations for both LAT(+) and LAT(−)A TG. In both LAT(+) and LAT(−)A virus-infected TG, the level of Tim-3 in gB^+ T cells was significantly higher than in gB^- T cells [51.4% versus 2% in LAT(+), with a *P* of 0.009 by a Students *t* test; 50% versus 1% in LAT(−)A, with a *P* of 0.0009 by a Student's *t* test). In contrast, this trend was reversed with PD-1, as we observed a higher number of $PD\text{-}1^+$ cells in gB^- T cells than in gB^+ T cells in both LAT(+) and LAT(−)A TG. Taken together, these results suggested that the level of $Tim\text{-}3^+$ is higher in gB^+ T cells while gB^- T cells have a larger amount of PD-1, and these patterns are similar between both LAT(+) and LAT(−)A virus-infected TG.

Levels of CD4, CD8-α, CD8-β, PD-1, Tim-3, IL-2, IL-21, IFN-γ, and TNF-α mRNAs in TG of mice latently infected with LAT(+) versus LAT(−)A virus. To investigate the effect of LAT on expression of T cell exhaustion markers and their related cytokines in TG of mice latently infected with HSV-1, C57BL/6 mice were infected as above with LAT(+) or LAT(−)A virus. The relative levels of several mRNAs for T cell subtypes (CD4 and CD8), markers of exhaustion (PD-1, Tim-3, and IL-21), and cytokines whose levels may be altered by exhaustion (IL-2, IFN-γ, and TNF-α) were determined by real-time PCR of total TG extracts. The results are presented as fold increase (or decrease) compared to the baseline mRNA levels in TG from uninfected naive mice (Fig. 5). In TG of mice latently infected with LAT(+) virus, the levels of CD4 (Fig. 5A), CD8-α (Fig. 5B), CD8-β (Fig. 5C), PD-1 (Fig. 5D), Tim-3

FIG. 2. Detection of $CD8^+$ $PD\text{-}1^+$ and $CD8^+$ $Tim\text{-}3^+$ T cells in TG of latently infected mice. C57BL/6 mice were infected in both eyes with 2×10^5 PFU/eye of LAT(+) or LAT(−)A virus. Naive mice were used as controls. At 30 days p.i., TG from five mice per group were harvested and digested with collagenase (400 IU/TG). The cell suspension was filtered through a 45-mm-pore-size cell strainer followed by a magnetic cell sorting (MACS) T cell isolation column and then stained with Pacific Blue-anti-CD8, FITC-anti-PD-1, and APC-anti-Tim-3 and analyzed by flow cytometry. Positive cells numbers are indicated in upper right corners of panels. (A) Representative histograms of $CD3^+$ $CD8^+$ T cells that are Tim-3 positive (left) or PD-1 positive (right) infected with LAT(+) virus from five pooled TG per group from four independent experiments. (B) Representative histograms of $CD3^+$ $CD8^+$ T cells that are Tim-3 positive (left) or PD-1 positive (right) infected with LAT(−)A virus from five pooled TG per group from four independent experiments. (C) Quantification of the mean number of $CD8^+$ $Tim\text{-}3^+$ (right) and $CD8^+$ $PD\text{-}1^+$ (left) T cells per individual TG in LAT(+) and LAT(−)A virus. The experiment was repeated four times for a total of 40 TG (20 mice/group), and values are means ± standard error of the means. (D) Representative histogram and dot blot for $CD3^+$ $CD4^+$ and $CD3^+$ $CD8^+$ T cells from the TG and spleen of naive mice.

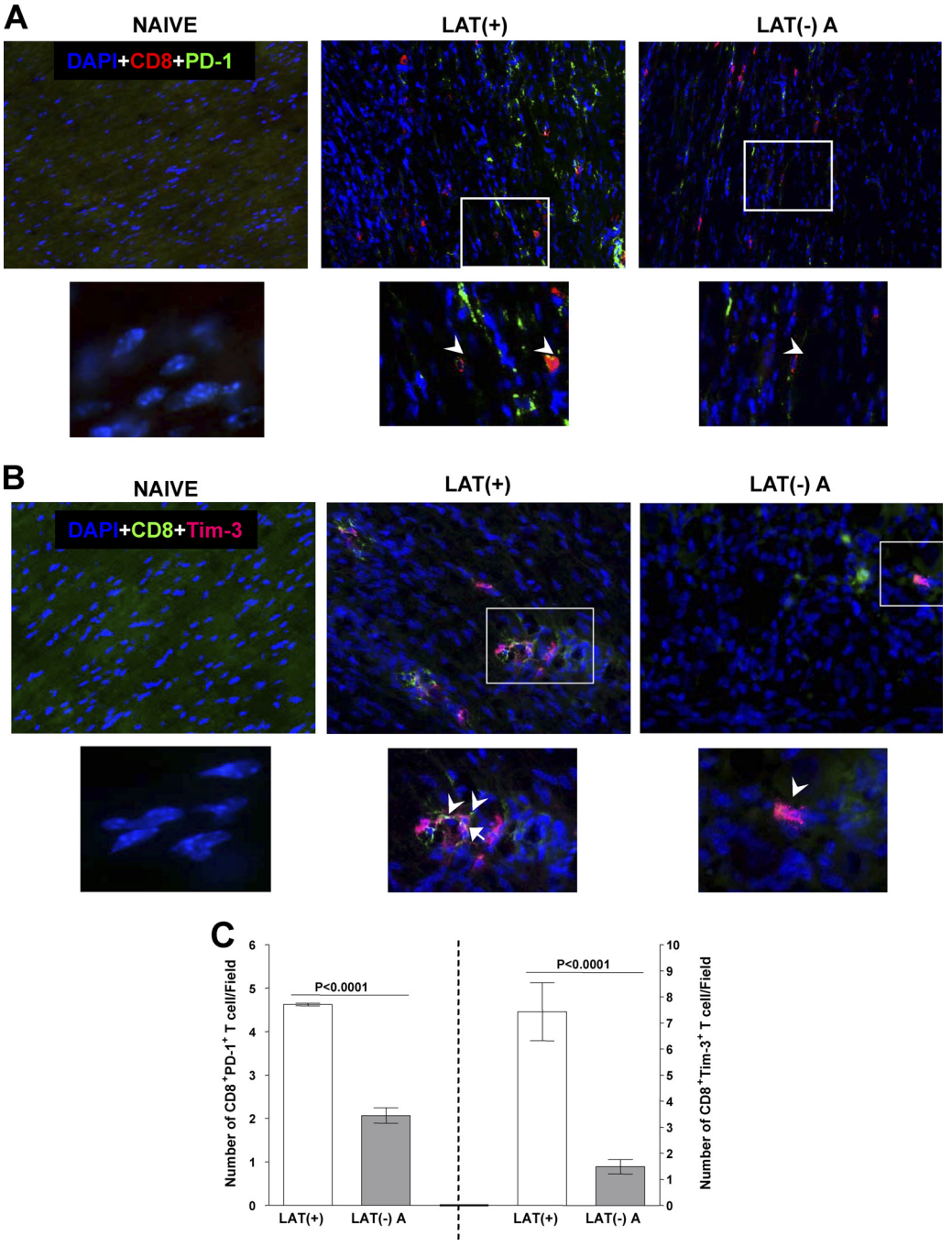

FIG. 3. Immunohistochemistry and quantification of $CD8^+$ T cell exhaustion markers in TG of latently infected mice. TG from 12 C57BL/6 mice latently infected with LAT(+) or LAT(−)A virus and 5 naive mice were isolated and stained with CD8, PD-1, and Tim-3 antibodies as described in Materials and Methods. (A) Representative photomicrographs of $CD8^+$ (Alexa Fluor-564; red) and $PD\text{-}1^+$ (Alexa Fluor-488; green) T cells in the TG of naïve mice and mice latently infected with LAT(+) and LAT(−) viruses. DAPI is shown as a nuclear counterstain. Arrows denote $CD8^+$ $PD\text{-}1^+$ T cells. (B) Representative photomicrographs of $CD8^+$ (Alexa Fluor-488; green) and $Tim\text{-}3^+$ (Alexa Fluor-647; red) T cells in the TG of naïve mice and mice latently infected with LAT(+) and LAT(−) viruses. DAPI is shown as a nuclear counterstain. Arrows denote $CD8^+$ $Tim\text{-}3^+$ T cells. (C) Quantification of photomicrographs. Different areas of each TG were imaged, and the number of double-positive cells was counted. Each point represents the mean ± standard error of the mean of $CD8^+$ $PD\text{-}1^+$ from 69 and 60 images for LAT(+) and LAT(−)A viruses, respectively, while each point for $CD8^+$ $Tim\text{-}3^+$ is from 20 and 34 images for LAT(+) and LAT(−)A viruses, respectively.

(Fig. 5E), IL-21 (Fig. 5F), IL-2 (Fig. 5G), IFN-γ (Fig. 5H), and TNF-α (Fig. 5I) mRNAs were all elevated over the uninfected baseline levels. In TG from mice latently infected with LAT(−)A virus, the levels of these mRNAs were either similar or slightly lower than baseline. For all of these mRNAs, the levels were significantly higher in the LAT(+) TG than in the LAT(−)A TG ($P < 0.0001$). These results suggest that there are both increased numbers of T cells and increased T cell

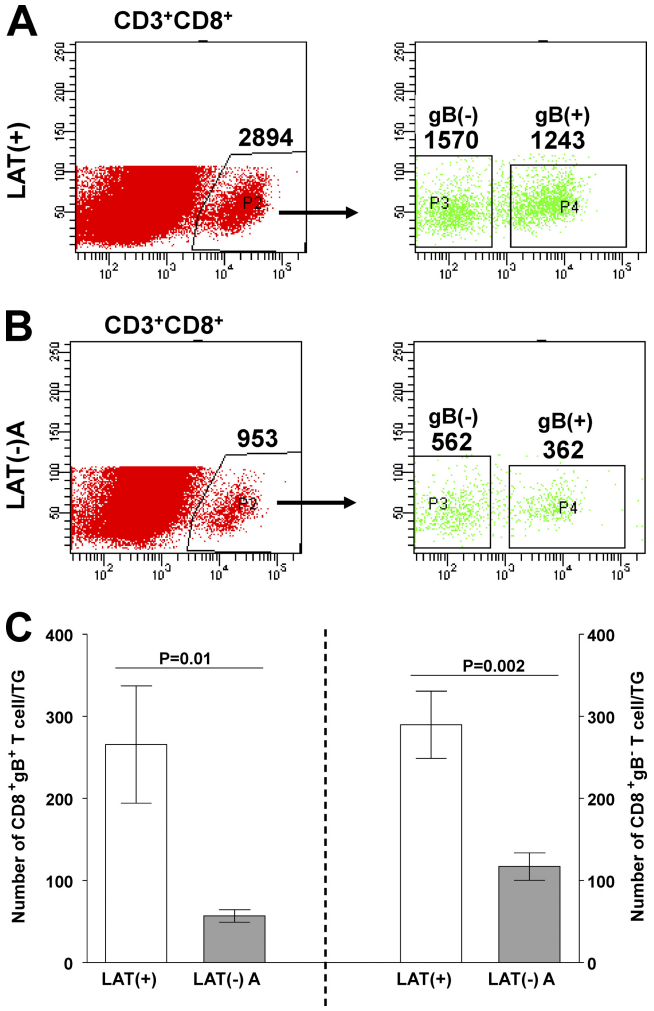

FIG. 4. Detection of $CD8^+$ gB^+ cells in TG of latently infected mice. TG from five mice latently infected with LAT(+) or LAT(−)A virus were combined, and total T cells were isolated as described in Materials and Methods. Total T cells were stained with Pacific Blue-anti-CD8 and PE-$gB_{498–505}$ pentamer and analyzed by FACS. (A) Representative histograms of $CD3^+$ $CD8^+$ T cells that are gB^+ or gB^- and infected with LAT(+) virus from five pooled TG. (B) Representative histograms of $CD3^+$ $CD8^+$ T cells that are gB^+ or gB^- and infected with LAT(−)A virus from five pooled TG. (C) Quantification of the mean number of $CD8^+$ gB^+ (left) and $CD8^+$ gB^- (right) T cells per TG of LAT(+) and LAT(−)A virus-infected mice from four separate experiments. Experiment was repeated four times for a total of 40 TG (20 mice/group); values are means ± standard error of the means.

exhaustion, as evidenced by increased expression of PD-1 and Tim-3 exhaustion markers in TG from mice latently infected with LAT(+) versus LAT(−)A viruses.

Functional impairment of CD8 and CD4 T cells from LAT(+) virus-infected TG. The above results (Fig. 2 to 5) suggested that the T cells from latently infected LAT(+) TG have more gB-specific, Tim-3- and PD-1-expressing T cells than LAT(−)A TG. To directly examine the functionality of these T cells, we looked at the total numbers of $CD4^+$ and $CD8^+$ T cells per individual mouse TG as well as the percentage of these T cells that are expressing the proinflammatory cytokines IL-2, TNF-α, and IFN-γ.

As expected, more $CD8^+$ T cells were detected per individual TG in the LAT(+) group than in the LAT(−)A group (377 ± 55 versus 173 ± 34 cells) (Table 2). The difference in CD8 expression between the LAT(+) and LAT(−)A groups was statistically significant (Student's *t* test, $P = 0.02$). In both LAT(+) and LAT(−)A TG, a small percentage of $CD8^+$ T cells produced IL-2 and TNF-α, while there appeared to be a higher percentage of IFN-γ-producing $CD8^+$ T cells in both LAT(+) and LAT(−)A groups, with a slight increase in the production by the LAT(−)A group over the LAT(+) group (Table 2). However, the differences between the LAT(+) and the LAT(−)A group did not quite reach statistical significance (Table 2). In contrast to the $CD8^+$ T cells, we observed a higher number of $CD4^+$ T cells per mouse TG in the LAT(−)A group than in the LAT(+) group, but these differences were not significant (Table 2). We also detected a trend of higher percentages of cytokine production by $CD4^+$ T cells in LAT(−)A T cells than in LAT(+) T cells (Table 2).

These results suggested that $CD8^+$ T cells in both LAT(+) and LAT(−)A TG show impairment in IL-2 and TNF-α cytokine production. Taken together with the increased expression of PD-1 and Tim-3, we can conclude that they are at least partially impaired.

Decreased latency in PD-1- and PD-L1-deficient, but not PD-L2 deficient, mice. Our results described above suggested a correlation between LAT(+) virus and elevated PD-1. Since LAT(+) virus results in more latency than LAT(−)A virus and since PD-1 is a marker of T cell exhaustion, the above results also suggested a correlation between increased latency and exhaustion. It was therefore of interest to determine the functional significance of high PD-1 expression ($PD\text{-}1^{high}$) during HSV latency. CD8 T cell exhaustion plays a major role in chronic infection with LCMV, and both PD-1 and its ligands are major markers of exhaustion and play a functional role in this exhaustion (5, 9, 79). *In vivo* administration of anti-PD-1 or anti-PD-L1 antibody that blocked the interaction of PD-1 with its ligand, PD-L1, enhanced T cell responses and clearance of LCMV (5), hepatitis C virus (HCV) (73), and HIV (66). Blocking or knockdown of PD-L2 in conjunction with PD-L1 was also shown to increase cytokine production by tumor-specific T cells *in vitro* (27) and by HCV-specific T cells (22). However, using the same blocking MAbs against PD-1, PD-L1, and PD-L2 as well as the same administration procedures, we did not detect any differences in the levels of latency between mock-treated and MAb-treated mice (data not shown). This lack of any biological effect could be due to inaccessibility of the TG by the antibody or to a repopulation of T cells after MAb administration was terminated on day 10 postinfection. Thus, to circumvent the potential pitfall associated with MAb administration, we used PD-1, PD-L1, and PD-L2 knockout mice. We hypothesized that in the absence of PD-1 or one or both of its ligands (i.e., in a situation in which CD8 T cell exhaustion is significantly reduced), HSV-1 latency would similarly be decreased. To test this, C57BL/6 $PD\text{-}1^{-/-}$ mice (PD-1-deficient mice), C57BL/6 $PD\text{-}L1^{-/-}$ mice (PD-L1-deficient mice), and parental wild-type C57BL/6 mice were infected ocularly as above with 2×10^5 PFU/eye of HSV-1 strain McKrae. At day 30 p.i., the amount of LAT RNA in TG of the latently infected mice was determined as described in Materials and Methods. LAT RNA was used as a marker for the

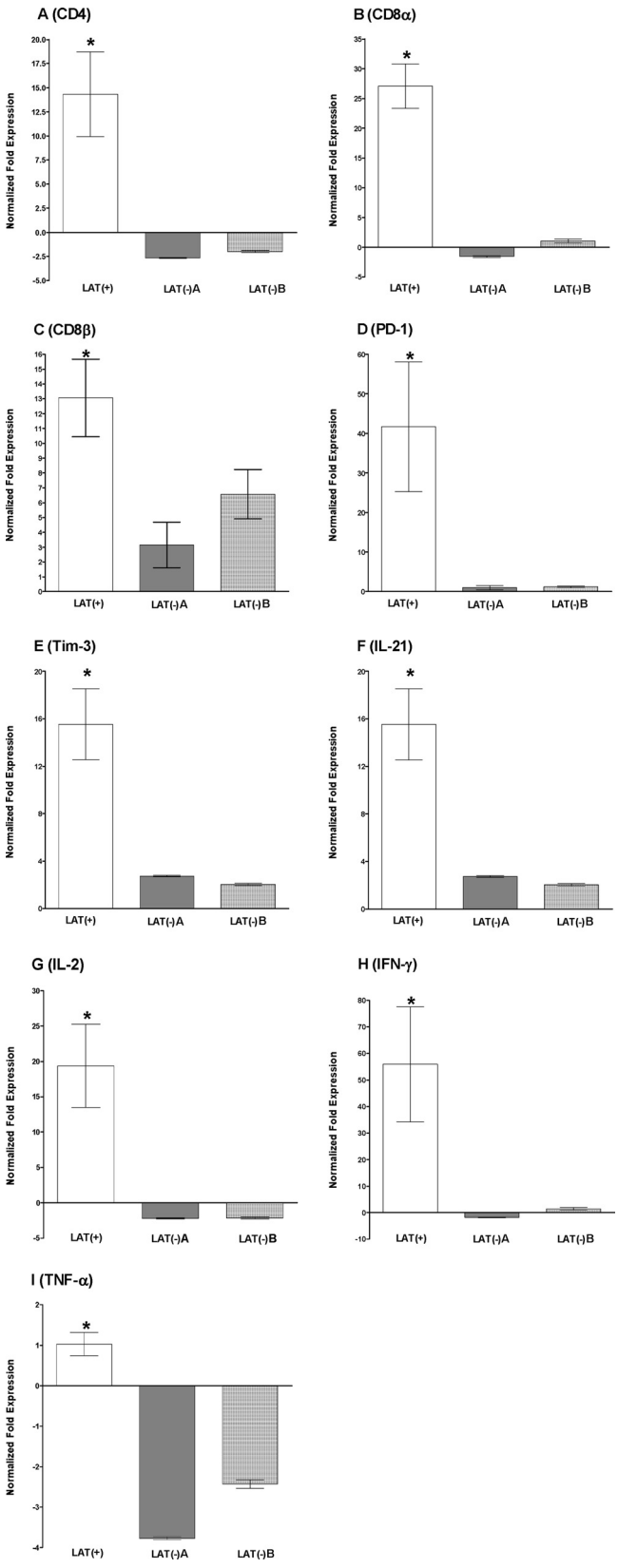

FIG. 5. Effect of LAT on various transcripts in TG of latently infected mice. TG from latently infected mice, infected as described in the legend of Fig. 1, were individually isolated on day 30 p.i., and quantitative RT-PCR was performed using total RNA as described in Materials and Methods. CD4, CD8-α, CD8-β, PD-1, Tim-3, IL-21, IL-2, IFN-γ, and TNF-α expression in naive mice was used as a baseline control to estimate the relative expression of each transcript in TG of latently infected mice. GAPDH expression was used to normalize the relative expression of each transcript. Each point represents the mean ± standard error of the mean from 20 TG. Transcripts are as indicated above each graph.

relative level of latent virus. The amount of HSV-1 LAT RNA in wt C57BL/6 mice appeared to be at least three times higher than that in PD-$1^{-/-}$ or PD-$L1^{-/-}$ mice (Fig. 6, left) ($P < 0.03$). The levels of LAT RNA were similarly low in the PD-$1^{-/-}$ and PD-$L1^{-/-}$ groups (Fig. 6, left) ($P = 0.4$). This suggested that PD-1 and PD-L1 are involved in the increase of latency.

The above studies suggest that both PD-1 and PD-L1 are involved in T cell exhaustion and increase of latency. To determine if, in addition to PD-L1, PD-L2 is also involved in increased latency, we also compared PD-$L1^{-/-}$ (PD-L1-deficient) and PD-$L2^{-/-}$ (PD-L2-deficient) mice with their wt control mice. These mice were from a BALB/c background and were infected ocularly with 2×10^4 PFU/eye of HSV-1 strain McKrae. At day 30 p.i., the amount of LAT RNA in TG of the latently infected mice was determined as described in Materials and Methods. The amount of HSV-1 LAT RNA in wt BALB/c and PD-$L2^{-/-}$ mice was significantly higher than in PD-$L1^{-/-}$ mice (Fig. 6, right) ($P < 0.0001$) while we detected no difference between PD-$L2^{-/-}$ and wt groups with respect to LAT RNA (Fig. 6, right) ($P > 0.5$). These results suggested that PD-L2 does not play a role in T cell exhaustion with regard to HSV-1 latency while the absence of PD-L1 reduced latency in two different strains of mice.

Detection of HSV-1 antigen in TG of latently infected mice. Continuous viral expression and antigen presentation are required to produce T cell exhaustion. Although LAT is the only consistently detected abundant HSV-1 transcript detected during latency, very low levels of other viral transcripts and proteins have been reported (15, 40). We sought to determine if we could also detect low-level viral protein expression and if there was a difference in potential Ag produced in TG from mice latently infected with LAT(+) virus versus LAT(−)A virus (which is also high versus low CD8 T cell exhaustion). Latently infected mice were prepared as described in the legend of Fig. 1. Briefly, TG were sectioned and stained with anti-MAP-2 neuronal marker and anti-HSV-1 FITC-conjugated polyclonal antibody. Three different layers of the TG were examined, and three consecutive sections from within each layer were screened to confirm results. Representative photomicrographs of TG infected with LAT(+) and LAT(−)A virus are presented in Fig. 7A (top and bottom panels, respectively), and HSV-1 Ag-positive neurons are indicated by arrows. Surface viral antigen was also detected in nearby cells of LAT(+) virus-infected TG (Fig. 7A, arrowhead in top panel). These surface HSV-1 antigens are absent in LAT(−)A TG (Fig. 7A, bottom panel). We detected 15 HSV-1 Ag-positive neurons in 23 individual LAT(+) TG and 3 HSV-1 Ag-positive neurons in 21 individual LAT(−)A TG. Quantification and statistical analysis revealed a frequency of 0.4 HSV-1 Ag-pos-

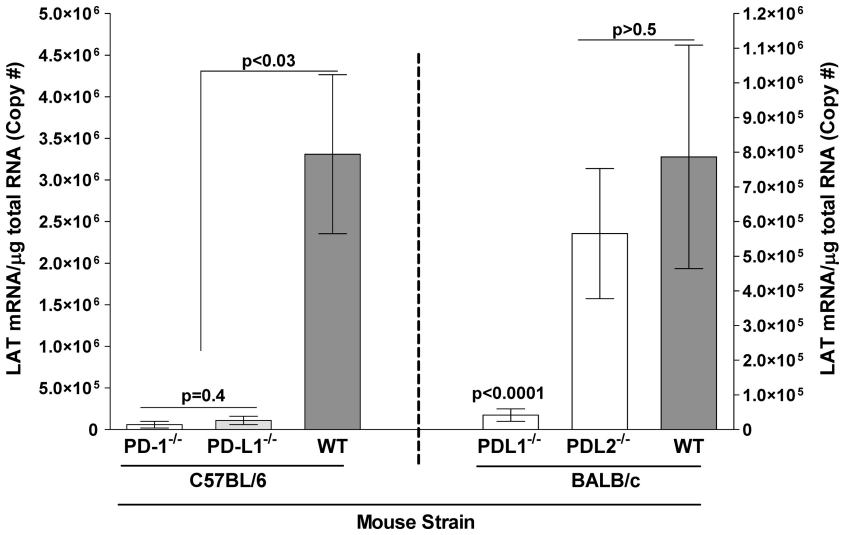

FIG. 6. Effect of PD-1, PD-L1, and PD-L2 deficiency on HSV-1 latency in TG of latently infected mice. C57BL/6 PD-1$^{-/-}$, C57BL/6 PD-L1$^{-/-}$, wt C57BL/6, BALB/c PD-L1$^{-/-}$, BALB/c PD-L2$^{-/-}$, and wt BALB/c mice were ocularly infected with HSV-1 strain McKrae [LAT(+)] as described in Materials and Methods. TG were harvested during latency on day 30 p.i., and quantitative RT-PCR was performed on individual TG for LAT expression. The estimated relative copy number of LAT was calculated using standard curves generated from pGem-5317, a LAT-containing plasmid. Briefly, DNA template was serially diluted 10-fold such that 5 μl contained from 10^3 to 10^{11} copies of LAT, and then samples were subjected to TaqMan PCR with the same set of primers. By comparing the normalized threshold cycle of each sample to the threshold cycle of the standard, the copy number for each reaction was determined. GAPDH expression was used to normalize the relative expression in the TG. Each point represents the mean ± standard error of the mean from 28, 20, 11, 9, and 11 TG in wt C57BL/6, C57BL/6 PD-1$^{-/-}$, C57BL/6 PD-L1$^{-/-}$, BALB/c PD-L1$^{-/-}$, BALB/c PD-L2$^{-/-}$, and wt BALB/c mice, respectively.

itive neurons per LAT(+) TG and 0.15 HSV-1 Ag-positive neurons per LAT(−)A TG (Fig. 7B) (P = 0.0001, Fisher's exact test). These results are consistent with a previously reported study for the number of HSV-1-positive neurons in latently infected mouse TG (42).

DISCUSSION

Chronic infections with HIV, hepatitis B virus (HBV), hepatitis C virus (HCV), and human T-lymphotropic virus (HTLV) generate functionally impaired antigen-specific T cell populations (21, 25, 37, 39). Functional exhaustion of CD8$^+$ T cells is well documented in chronic lymphocytic choriomeningitis virus (LCMV) infection of mice (5, 37, 79). PD-1 is a key mediator of T cell exhaustion during chronic LCMV infection (5). PD-1 is expressed on the surface of activated T cells, macrophages, and B cells and on some dendritic cells (DCs) (1, 37). Following ligation of its ligands, PD-L1 and PD-L2, PD-1 inhibits activation, expansion, and acquisition of CD8 T cell effector function (5). Thus, PD-1 on the surface of CD8 T cells leads to exhaustion and is also a useful marker of exhaustion (37).

Previously, it was reported that CD8 T cell exhaustion occurs as a result of long-term (5 to 7 days), continuous exposure of virus-specific T cells to viral Ag (37, 50). Removal of Ag even for a short period (24 h) results in rapid recovery, decreased PD-1 expression, and lack of exhaustion (37, 50). The length of Ag exposure that was needed to exhaust the T cell initially is also required for the same CD8 T cell to return to an exhausted state. Thus, CD8 T cell exhaustion is an exquisitely sensitive indicator of continuous exposure to the Ag. Based on this simple explanation, exhaustion is consistent with a chronic viral infection in which low-level Ag is continuously present. In contrast, for a virus with tight (i.e., nonleaky) latency, such as HSV-1 in mice, where spontaneous reactivation does not occur (81) or occurs very rarely (15, 42), exhaustion would not be expected. HSV-1 latency was originally thought to be a completely dormant situation with no viral gene expression, except when spontaneous reactivation was occurring. With the discovery of LAT RNA, which is abundantly expressed throughout latency, HSV-1 latency was still thought to be a dormant situation with the exception of LAT. The advent of more sensitive molecular tools has enabled detection of small amounts of other viral gene products in a small number of "latently" infected neurons in mice in a small fraction of the TG examined (15, 40, 42). In this study we detected viral antigens in few neurons from LAT(+) TG and significantly less Ag from LAT(−) TG during latency. These findings suggest either that low-level expression of viral Ags occurs in a small number of neurons during latency or that subclinical or abortive reactivations occur in mice at very low levels.

In the case of abortive reactivations, significant CD8 T cell exhaustion would not be expected in all latently infected mouse TG examined, as we found here, unless the abortive reactivations were occurring continuously in all of these TG. This is not thought to occur as current molecular techniques detect only low levels of viral Ag in a small fraction of neurons in a small fraction of mouse TG. Thus, the CD8 T cell exhaustion seen in this report suggests continuous low-level expression of one or more viral Ags in the entire mouse TG during HSV-1 latency. This finding suggests a shift in dogma about HSV-1 latency. Rather than a dormant infection (except when spontaneous reactivation is occurring), HSV latency appears to be a very

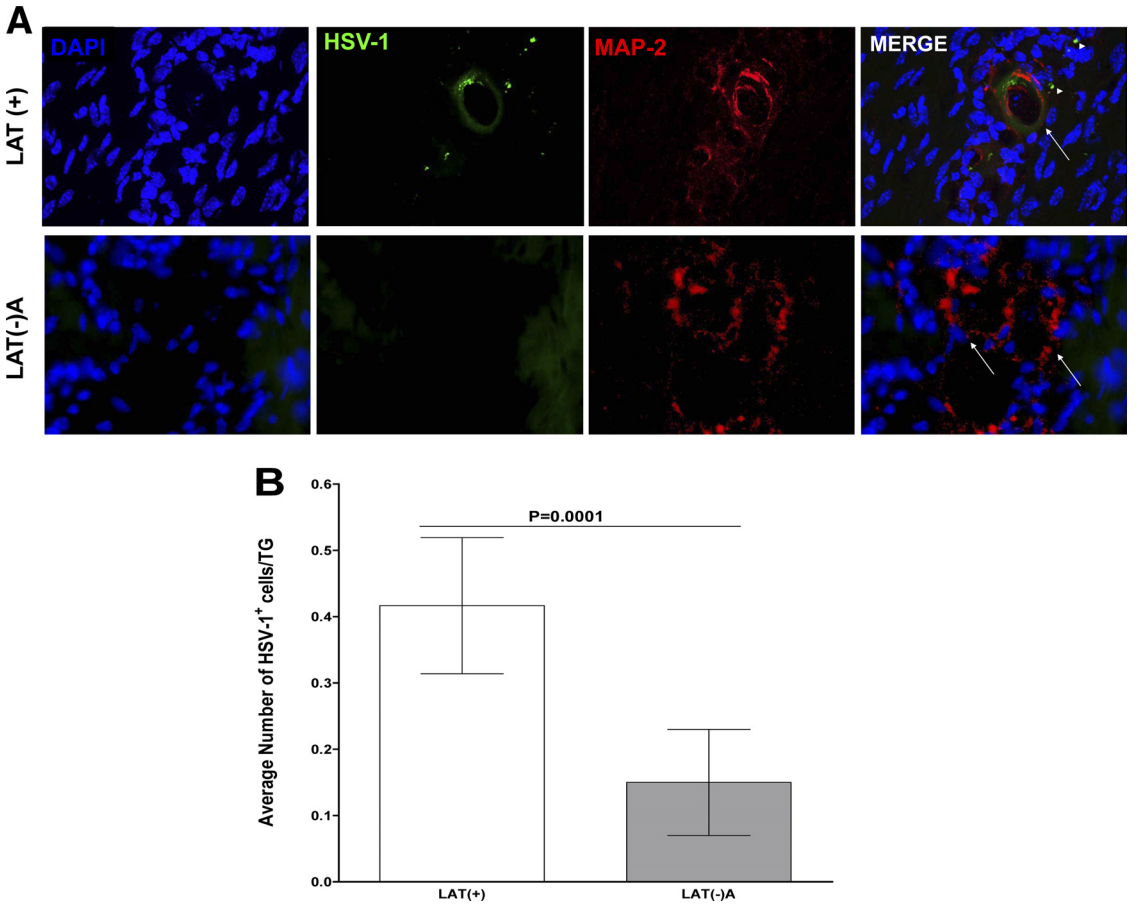

FIG. 7. Detection of HSV-1 antigen in neurons of latently infected mice. C57BL/6 mice were ocularly infected with LAT(+) and LAT(−)A viruses as described in the legend of Fig. 1. TG from infected mice on day 30 p.i. were stained with MAP-2 and HSV FITC-conjugated antibodies, and presence of viral antigen was monitored by confocal microscopy as described in Materials and Methods. (A) Staining of LAT(+) and LAT(−)A TG, as indicated. Columns in respective order show DAPI nuclear staining (blue), HSV-gC expression in the TG (green), MAP-2 neuronal marker (red), and merged images of DAPI, FITC, and Alexa Fluor-647 images. Arrows indicate HSV-1-positive neurons, and arrowheads indicate HSV-1 viral antigen on the cell surface. (B) Quantification of photomicrographs. Sections from the entire TG were imaged, and the numbers of HSV-positive neurons were counted. Each point represents the mean ± standard error of the mean using multiple sections from 23 and 21 LAT(+) and LAT(−)A TG, respectively.

low-level chronic infection or perhaps a mixture of true latency in some neurons and low-level chronic infection in others.

Alternative explanations exist. CD8 T cell exhaustion is an exquisitely sensitive measure of exposure to Ag, presumably much more sensitive than any current molecular techniques. Thus, there may be a low level of continuous abortive reactivation attempts occurring in all TG of latently infected mice that is below the level of detection using antibodies or RT-PCR but that is sufficient to maintain significant CD8 T cell exhaustion. Alternatively, there may be a low-level chronic infection that cannot be detected by molecular techniques but that produces enough viral Ag to maintain CD8 T cell exhaustion. It is also possible that LAT, which is continuously expressed in all TG of mice latently infected with an LAT(+) virus, or some other aspect of the latent infection may induce continued expression of a cellular Ag that directly or indirectly results in CD8 T cell exhaustion. Sustained antigen presentation by antigen-presenting cells (APCs) present in the TG may be involved; these APCs survive for extended periods, as we have previously shown that these APCs can be infected by HSV-1 but are resistant to HSV-1 replication (49). Thus, these APCs may continue to present viral Ag to the CD8 T cells for extended periods (i.e., months), and this may be sufficient to cause CD8 T cell exhaustion even in the complete absence of any other source of viral Ag. Finally, LAT may encode a protein that drives CD8 T cell exhaustion in TG from mice latently infected with LAT(+) virus. Theories about extended antigen presentation or low-level antigen production by low-level infection are supported by the visualization of cellular surface viral antigen (Fig. 7A, merge panel) in LAT(+), but not LAT(−), TG.

Recent studies have shown that T cell exhaustion occurs as a result of chronic infection with several different viruses (5, 10, 37). Previously, we found that in mice latently infected with wild-type [LAT(+)] HSV-1, the TG with more LAT RNA (and thus presumably more latency and more reactivation potential) tended to have more PD-1 mRNA (45), suggesting more severe T cell exhaustion. We have also shown in this report that there is a correlation between the presence of LAT and expression of T cell exhaustion markers and overall reduced

TNF-α and IL-2 cytokine production signifying T cell exhaustion. Since there is more latency with LAT(+) than with LAT(−) viruses, there is also a correlation between more latency and more CD8 T cell marker expression. This raised the question as to whether increased HSV-1 latency is a cause or a consequence of CD8 T cell exhaustion. We found here that in PD-$1^{-/-}$ and PD-$L1^{-/-}$ mice, the amount of latency following infection with wild-type [LAT(+)] virus was significantly reduced compared to that in wild-type C57BL/6 mice. This suggests that T cell responses and viral clearance are enhanced in LAT(+) virus-infected PD-$1^{-/-}$ and PD-$L1^{-/-}$ mice but not PD-$L2^{-/-}$ mice. Consistent with this hypothesis, PD-$L1^{-/-}$ mice die following infection with LCMV clone 13, which causes chronic infection, but exhibit increased T cell responses and viral clearance (5, 51, 79). These findings suggest that decreased CD8 T cell exhaustion results in decreased latency and that fully functional CD8 T cells in the TG play a role in decreasing the amount of HSV-1 latency that is established and/or maintained in the TG following ocular infection. In this study we have shown that both Tim-3 and PD-1 are also expressed on $CD4^+$ T cells. Thus, our results may suggest that higher Tim-3 as well as PD-1 activities may be associated with reduced $CD4^+$ T cell help for $CD8^+$ T cells, and this may lead to higher latency. In line with this, we have previously shown that the level of HSV-1 latency in $CD4^{-/-}$ mice was significantly higher than that in wt mice (48). Also consistent with our results is the finding that expression of Tim-3 and PD-1 on $CD4^+$ T cells can reduce their function (3, 16).

Recent studies have now demonstrated that in addition to PD-1, upregulation of Tim-3 (T cell immunoglobulin and mucin domain-containing protein 3) is correlated with T cell exhaustion (23, 30, 33). In this study we found that, similar to PD-1, upregulation of Tim-3 was correlated with increased HSV-1 latency. Tim-3 is an inhibitory molecule that terminates T_h1 immunity (64, 65). Our observation of a combined effort by Tim-3 and PD-1 to produce exhausted T cells is in line with recent studies where the coexpression of both exhaustion markers was associated with more severe T cell exhaustion in chronic LCMV infection (30), in chronic HIV/HCV coinfection (74), and in melanoma patients (17). Interestingly, we did observe that both PD-1 and PD-L1 expression had a negative effect on Tim-3 expression (data not shown). This result suggests that PD-1 and Tim-3 are involved in a synergistic way, which would support the additive effect that both exhaustion markers had on CD8 T cell function, as was recently reported for LCMV infection (30), HIV/HCV coinfection (74), and antitumor immunity (17, 67). Similarly, in this study we observed increased expression of Tim-3 on gB-positive (HSV-specific) T cells and increased expression of PD-1 on gB-negative T cells. This demonstrates an important role for both PD-1 and Tim-3 in relation to disease progression and pathology caused by T cells. This increased expression of exhaustion markers is also in line with a recent study in which we have shown that the level of Tim-3/PD-1 expression on T cells can be altered by immunization (4). In addition to PD-1 and Tim-3, it was recently shown that the absence of IL-21 or IL-21 receptor also contributed to T cell exhaustion (13, 20, 82). However, in this study we did not find any correlation between IL-21 expression and HSV-1 latency.

It has been shown that during chronic infection there is a loss of T cell function in which cytotoxic T cells (CTL) lose the ability to produce IL-2, TNF-α, and IFN-γ (78, 83). Similarly, in this study we have shown that few $CD8^+$ T cells produced IL-2 and TNF-α in TG of both LAT(+) and LAT(−) virus-infected mice. However, many $CD8^+$ T cells produced IFN-γ in both LAT(+) and LAT(−) TG. Previously, we have shown that LAT levels in IFN-$\gamma^{-/-}$ mice were similar to those of wt C57BL/6 mice (48), suggesting that IFN-γ is not involved in protection from latency. Furthermore, in mouse models of systemic lupus erythematosus, it has been shown that PD-1^{high} T cells are dysfunctional and yet retain the ability to produce excessive amounts of IFN-γ (35). These observations are also in line with exhaustion studies that demonstrated that loss of IFN-γ production was a final impairment before deletion (78). Also similar to our results was a report showing that IFN-γ participated in upregulation of PD-1 expression and, thus, inhibition of T cell effector functions (34). There are other studies that have shown a lack of correlation of T cell exhaustion and lower IL-2 and IFN-γ responses (10, 59, 60, 72). The differences between IL-2, TNF-α, and IFN-γ expression in different studies may be due to the use of different viruses. However, our results presented here may suggest that increased PD-1 and Tim-3 expression and T cell exhaustion are correlated with decreased IL-2 and TNF-α production by T cells. It should be noted that the increase of inflammatory cytokine transcripts we observed and the lack of protein detected could be due to a blockade of translation mediated by HSV-1 as a means of immune evasion. It is advantageous for the virus to encourage cellular machinery to increase the production of needed elements and inhibit the production of elements that would increase recognition and elimination by immune cells. This effect of cytokine inhibition via translational blockade has been demonstrated most clearly with respect to reduction of IFN-γ production by HSV-1 ICP0 and ICP34.5 (44). The alternate explanation exists that the observed increase in expression is caused by other immune cells (i.e., NK or B cells or macrophages) and is not a direct product of T cells.

Overall, our results suggest that LAT expression directly or indirectly results in increased CD8 T cell levels and increased CD8 T cell exhaustion in TG during latency. This may be due to the increased levels of latency with LAT(+) versus LAT(−) virus, which results in more exposure of CD8 T cells to viral Ag, leading to increased PD-1/Tim-3 and CD8 T cell exhaustion. Finally, our results also suggest the possibility that there are three populations of exhausted CD8 T cells in the TG of latently infected mice, one expressing PD-1, one expressing Tim-3, and one expressing both PD-1 and Tim-3.

ACKNOWLEDGMENTS

This work was supported by PHS grants EY13615 (H.G.) and EY13191 (S.L.W.), The Discovery Eye Foundation, The Henry L. Guenther Foundation, Research to Prevent Blindness, and grant P01 56299 to A.H.S., G.J.F., and R.A. S.L. Wechsler is an RPB Senior Scientific Investigator. Support was also provided by the USDA Agriculture and Food Research Initiative Competitive Grants Program (08-00891 and 09-01653) and a PHS grant to the Nebraska Center for Virology (1P20RR15635).

REFERENCES

1. **Agata, Y., et al.** 1996. Expression of the PD-1 antigen on the surface of stimulated mouse T and B lymphocytes. Int. Immunol. **8:**765–772.

2. **Ahmed, M., and N. W. Fraser.** 2001. Herpes simplex virus type 1 2-kilobase latency-associated transcript intron associates with ribosomal proteins and splicing factors. J. Virol. **75:**12070–12080.
3. **Albareda, M. C., et al.** 2009. Chronic human infection with *Trypanosoma cruzi* drives $CD4^+$ T cells to immune senescence. J. Immunol. **183:**4103–4108.
4. **Allen, S. J., K. R. Mott, M. Zandian, and H. Ghiasi.** 2010. Immunization with different viral antigens alters the pattern of T cell exhaustion and latency in HSV-1 infected mice. J. Virol. **84:**12315–12324.
5. **Barber, D. L., et al.** 2006. Restoring function in exhausted CD8 T cells during chronic viral infection. Nature **439:**682–687.
6. **Barron, B. A., et al.** 1994. Herpetic Eye Disease Study. A controlled trial of oral acyclovir for herpes simplex stromal keratitis. Ophthalmology **101:**1871–1882.
7. **Branco, F. J., and N. W. Fraser.** 2005. Herpes simplex virus type 1 latency-associated transcript expression protects trigeminal ganglion neurons from apoptosis. J. Virol. **79:**9019–9025.
8. **Carpenter, D., et al.** 2007. Stable cell lines expressing high levels of the herpes simplex virus type 1 LAT are refractory to caspase 3 activation and DNA laddering following cold shock induced apoptosis. Virology **369:**12–18.
9. **Chen, J., et al.** 2011. Intrahepatic levels of PD-1/PD-L correlate with liver inflammation in chronic hepatitis B. Inflamm. Res. **60:**47–53.
10. **Day, C. L., et al.** 2006. PD-1 expression on HIV-specific T cells is associated with T-cell exhaustion and disease progression. Nature **443:**350–354.
11. **Derfuss, T., V. Arbusow, M. Strupp, T. Brandt, and D. Theil.** 2009. The presence of lytic HSV-1 transcripts and clonally expanded T cells with a memory effector phenotype in human sensory ganglia. Ann. N. Y. Acad. Sci. **1164:**300–304.
12. **Dix, R. D.** 2002. Pathogenesis of herpes simplex ocular disease, vol. 2. Lippincott, Williams and Wilkins, Philadelphia, PA.
13. **Elsaesser, H., K. Sauer, and D. G. Brooks.** 2009. IL-21 is required to control chronic viral infection. Science **324:**1569–1572.
14. **Farrell, M. J., A. T. Dobson, and L. T. Feldman.** 1991. Herpes simplex virus latency-associated transcript is a stable intron. Proc. Natl. Acad. Sci. U. S. A. **88:**790–794.
15. **Feldman, L. T., et al.** 2002. Spontaneous molecular reactivation of herpes simplex virus type 1 latency in mice. Proc. Natl. Acad. Sci. U. S. A. **99:**978–983.
16. **Fletcher, J. M., et al.** 2005. Cytomegalovirus-specific $CD4^+$ T cells in healthy carriers are continuously driven to replicative exhaustion. J. Immunol. **175:**8218–8225.
17. **Fourcade, J., et al.** 2010. Upregulation of Tim-3 and PD-1 expression is associated with tumor antigen-specific $CD8^+$ T cell dysfunction in melanoma patients. J. Exp. Med. **207:**2175–2186.
18. **Fraser, N. W., et al.** 1991. A review of the molecular mechanism of HSV-1 latency. Curr. Eye Res. **10:**1–13.
19. **Fraser, N. W., and T. Valyi-Nagy.** 1993. Viral, neuronal and immune factors which may influence herpes simplex virus (HSV) latency and reactivation. Microb. Pathog. **15:**83–91.
20. **Frohlich, A., et al.** 2009. IL-21R on T cells is critical for sustained functionality and control of chronic viral infection. Science **324:**1576–1580.
21. **Goepfert, P. A., et al.** 2000. A significant number of human immunodeficiency virus epitope-specific cytotoxic T lymphocytes detected by tetramer binding do not produce gamma interferon. J. Virol. **74:**10249–10255.
22. **Golden-Mason, L., et al.** 2007. Upregulation of PD-1 expression on circulating and intrahepatic hepatitis C virus-specific $CD8^+$ T cells associated with reversible immune dysfunction. J. Virol. **81:**9249–9258.
23. **Golden-Mason, L., et al.** 2009. Negative immune regulator Tim-3 is overexpressed on T cells in hepatitis C virus infection and its blockade rescues dysfunctional $CD4^+$ and $CD8^+$ T cells. J. Virol. **83:**9122–9130.
24. **Gordon, Y. J.** 1990. Pathogenesis and latency of herpes simplex virus type 1 (HSV-1): an ophthalmologist's view of the eye as a model for the study of the virus-host relationship. Adv. Exp. Med. Biol. **278:**205–209.
25. **Gruener, N. H., et al.** 2001. Sustained dysfunction of antiviral $CD8^+$ T lymphocytes after infection with hepatitis C virus. J. Virol. **75:**5550–5558.
26. **Hill, J. M., F. Sedarati, R. T. Javier, E. K. Wagner, and J. G. Stevens.** 1990. Herpes simplex virus latent phase transcription facilitates in vivo reactivation. Virology **174:**117–125.
27. **Hobo, W., et al.** 2010. siRNA silencing of PD-L1 and PD-L2 on dendritic cells augments expansion and function of minor histocompatibility antigen-specific $CD8^+$ T cells. Blood **116:**4501–4511.
28. **Hufner, K., et al.** 2009. Fewer latent herpes simplex virus type 1 and cytotoxic T cells occur in the ophthalmic division than in the maxillary and mandibular divisions of the human trigeminal ganglion and nerve. J. Virol. **83:**3696–3703.
29. **Inman, M., et al.** 2001. Region of herpes simplex virus type 1 latency-associated transcript sufficient for wild-type spontaneous reactivation promotes cell survival in tissue culture. J. Virol. **75:**3636–3646.
30. **Jin, H. T., et al.** 2010. Cooperation of Tim-3 and PD-1 in CD8 T-cell exhaustion during chronic viral infection. Proc. Natl. Acad. Sci. U. S. A. **107:**14733–14738.
31. **Jin, L., et al.** 2003. Identification of herpes simplex virus type 1 latency-associated transcript sequences that both inhibit apoptosis and enhance the spontaneous reactivation phenotype. J. Virol. **77:**6556–6561.
32. **Jin, L., et al.** 2007. Reactivation phenotype in rabbits of a herpes simplex virus type 1 mutant containing an unrelated antiapoptosis gene in place of latency-associated transcript. J. Neurovirol. **13:**78–84.
33. **Jones, R. B., et al.** 2008. Tim-3 expression defines a novel population of dysfunctional T cells with highly elevated frequencies in progressive HIV-1 infection. J. Exp. Med. **205:**2763–2779.
34. **Jurado, J. O., et al.** 2008. Programmed death (PD)-1:PD-ligand 1/PD-ligand 2 pathway inhibits T cell effector functions during human tuberculosis. J. Immunol. **181:**116–125.
35. **Kasagi, S., et al.** 2010. Anti-programmed cell death 1 antibody reduces $CD4^+$ $PD\text{-}1^+$ T cells and relieves the lupus-like nephritis of NZB/W F1 mice. J. Immunol. **184:**2337–2347.
36. **Kaufman, H. E., et al.** 2005. HSV-1 DNA in tears and saliva of normal adults. Invest. Ophthalmol. Vis. Sci. **46:**241–247.
37. **Keir, M. E., M. J. Butte, G. J. Freeman, and A. H. Sharpe.** 2008. PD-1 and its ligands in tolerance and immunity. Annu. Rev. Immunol. **26:**677–704.
38. **Keir, M. E., et al.** 2006. Tissue expression of PD-L1 mediates peripheral T cell tolerance. J. Exp. Med. **203:**883–895.
39. **Klenerman, P., and A. Hill.** 2005. T cells and viral persistence: lessons from diverse infections. Nat. Immunol. **6:**873–879.
40. **Kramer, M. F., and D. M. Coen.** 1995. Quantification of transcripts from the ICP4 and thymidine kinase genes in mouse ganglia latently infected with herpes simplex virus. J. Virol. **69:**1389–1399.
41. **Latchman, Y. E., et al.** 2004. PD-L1-deficient mice show that PD-L1 on T cells, antigen-presenting cells, and host tissues negatively regulates T cells. Proc. Natl. Acad. Sci. U. S. A. **101:**10691–10696.
42. **Margolis, T. P., et al.** 2007. Spontaneous reactivation of herpes simplex virus type 1 in latently infected murine sensory ganglia. J. Virol. **81:**11069–11074.
43. **McGeoch, D. J., et al.** 1988. The complete DNA sequence of the long unique region in the genome of herpes simplex virus type 1. J. Gen. Virol. **69:**1531–1574.
44. **Mossman, K. L., and J. R. Smiley.** 2002. Herpes simplex virus ICP0 and ICP34.5 counteract distinct interferon-induced barriers to virus replication. J. Virol. **76:**1995–1998.
45. **Mott, K. R., et al.** 2009. Level of herpes simplex virus type 1 latency correlates with severity of corneal scarring and exhaustion of $CD8^+$ T cells in trigeminal ganglia of latently infected mice. J. Virol. **83:**2246–2254.
46. **Mott, K. R., et al.** 2007. The corneas of naive mice contain both $CD4^+$ and $CD8^+$ T cells. Mol. Vis. **13:**1802–1812.
47. **Mott, K. R., G. C. Perng, Y. Osorio, K. G. Kousoulas, and H. Ghiasi.** 2007. A recombinant herpes simplex virus type 1 expressing two additional copies of gK is more pathogenic than wild-type virus in two different strains of mice. J. Virol. **81:**12962–12972.
48. **Mott, K. R., D. UnderHill, S. L. Wechsler, and H. Ghiasi.** 2008. Lymphoid-related $CD11c^+$ $CD8a^+$ dendritic cells are involved in enhancing HSV-1 latency. J. Virol. **82:**9870–9879.
49. **Mott, K. R., D. Underhill, S. L. Wechsler, T. Town, and H. Ghiasi.** 2009. A role for the JAK-STAT1 pathway in blocking replication of HSV-1 in dendritic cells and macrophages. Virol. J. **6:**56.
50. **Mueller, S. N., and R. Ahmed.** 2009. High antigen levels are the cause of T cell exhaustion during chronic viral infection. Proc. Natl. Acad. Sci. U. S. A. **106:**8623–8628.
51. **Mueller, S. N., et al.** 2010. PD-L1 has distinct functions in hematopoietic and nonhematopoietic cells in regulating T cell responses during chronic infection in mice. J. Clin. Invest. **120:**2508–2515.
52. **Nicosia, M., J. M. Zabolotny, R. P. Lirette, and N. W. Fraser.** 1994. The HSV-1 2-kb latency-associated transcript is found in the cytoplasm comigrating with ribosomal subunits during productive infection. Virology **204:**717–728.
53. **Osorio, Y., and H. Ghiasi.** 2003. Comparison of adjuvant efficacy of herpes simplex virus type 1 recombinant viruses expressing TH1 and TH2 cytokine genes. J. Virol. **77:**5774–5783.
54. **Peng, W., et al.** 2004. Mapping herpes simplex virus type 1 latency-associated transcript sequences that protect from apoptosis mediated by a plasmid expressing caspase-8. J. Neurovirol. **10:**260–265.
55. **Perng, G. C., et al.** 1994. The latency-associated transcript gene of herpes simplex virus type 1 (HSV-1) is required for efficient in vivo spontaneous reactivation of HSV-1 from latency. J. Virol. **68:**8045–8055.
56. **Perng, G. C., et al.** 2000. Virus-induced neuronal apoptosis blocked by the herpes simplex virus latency-associated transcript. Science **287:**1500–1503.
57. **Perng, G. C., et al.** 2002. A gene capable of blocking apoptosis can substitute for the herpes simplex virus type 1 latency-associated transcript gene and restore wild-type reactivation levels. J. Virol. **76:**1224–1235.
58. **Perng, G. C., et al.** 2000. The latency-associated transcript gene enhances establishment of herpes simplex virus type 1 latency in rabbits. J. Virol. **74:**1885–1891.
59. **Petrovas, C., et al.** 2006. PD-1 is a regulator of virus-specific $CD8^+$ T cell survival in HIV infection. J. Exp. Med. **203:**2281–2292.
60. **Petrovas, C., et al.** 2007. SIV-specific $CD8^+$ T cells express high levels of

PD1 and cytokines but have impaired proliferative capacity in acute and chronic SIVmac251 infection. Blood **110:**928–936.
61. **Remeijer, L., J. Maertzdorf, P. Doornenbal, G. M. Verjans, and A. D. Osterhaus.** 2001. Herpes simplex virus 1 transmission through corneal transplantation. Lancet **357:**442.
62. **Robert, P. Y., J. P. Adenis, F. Denis, S. Alain, and S. Ranger-Rogez.** 2003. Herpes simplex virus DNA in corneal transplants: prospective study of 38 recipients. J. Med. Virol. **71:**69–74.
63. **Rock, D. L., et al.** 1987. Detection of latency-related viral RNAs in trigeminal ganglia of rabbits latently infected with herpes simplex virus type 1. J. Virol. **61:**3820–3826.
64. **Rodriguez-Manzanet, R., R. DeKruyff, V. K. Kuchroo, and D. T. Umetsu.** 2009. The costimulatory role of TIM molecules. Immunol. Rev. **229:**259–270.
65. **Sabatos, C. A., et al.** 2003. Interaction of Tim-3 and Tim-3 ligand regulates T helper type 1 responses and induction of peripheral tolerance. Nat. Immunol. **4:**1102–1110.
66. **Sachdeva, M., M. A. Fischl, R. Pahwa, N. Sachdeva, and S. Pahwa.** 2010. Immune exhaustion occurs concomitantly with immune activation and decrease in regulatory T cells in viremic chronically HIV-1-infected patients. J. Acquir. Immune Defic. Syndr. **54:**447–454.
67. **Sakuishi, K., et al.** 2010. Targeting Tim-3 and PD-1 pathways to reverse T cell exhaustion and restore anti-tumor immunity. J. Exp. Med. **207:**2187–2194.
68. **Sawtell, N. M.** 1997. Comprehensive quantification of herpes simplex virus latency at the single-cell level. J. Virol. **71:**5423–5431.
69. **Sawtell, N. M., D. K. Poon, C. S. Tansky, and R. L. Thompson.** 1998. The latent herpes simplex virus type 1 genome copy number in individual neurons is virus strain specific and correlates with reactivation. J. Virol. **72:**5343–5350.
70. **Steiner, I.** 1996. Human herpes viruses latent infection in the nervous system. Immunol. Rev. **152:**157–173.
71. **Stevens, J. G.** 1989. Human herpesviruses: a consideration of the latent state. Microbiol. Rev. **53:**318–332.
72. **Trautmann, L., et al.** 2006. Upregulation of PD-1 expression on HIV-specific $CD8^+$ T cells leads to reversible immune dysfunction. Nat. Med. **12:**1198–1202.
73. **Urbani, S., et al.** 2006. PD-1 expression in acute hepatitis C virus (HCV) infection is associated with HCV-specific CD8 exhaustion. J. Virol. **80:**11398–11403.
74. **Vali, B., et al.** 2010. HCV-specific T cells in HCV/HIV co-infection show elevated frequencies of dual Tim-3/PD-1 expression that correlate with liver disease progression. Eur. J. Immunol. **40:**2493–2505.
75. **Wagner, E. K., et al.** 1988. The herpes simplex virus latency-associated transcript is spliced during the latent phase of infection. J. Virol. **62:**4577–4585.
76. **Wechsler, S. L., A. B. Nesburn, R. Watson, S. Slanina, and H. Ghiasi.** 1988. Fine mapping of the major latency-related RNA of herpes simplex virus type 1 in humans. J. Gen. Virol. **69:**3101–3106.
77. **Wechsler, S. L., A. B. Nesburn, R. Watson, S. M. Slanina, and H. Ghiasi.** 1988. Fine mapping of the latency-related gene of herpes simplex virus type 1: alternative splicing produces distinct latency-related RNAs containing open reading frames. J. Virol. **62:**4051–4058.
78. **Wherry, E. J., J. N. Blattman, K. Murali-Krishna, R. van der Most, and R. Ahmed.** 2003. Viral persistence alters CD8 T-cell immunodominance and tissue distribution and results in distinct stages of functional impairment. J. Virol. **77:**4911–4927.
79. **Wherry, E. J., et al.** 2007. Molecular signature of CD8+ T cell exhaustion during chronic viral infection. Immunity **27:**670–684.
80. **Wilhelmus, K. R., et al.** 1996. Risk factors for herpes simplex virus epithelial keratitis recurring during treatment of stromal keratitis or iridocyclitis. Herpetic Eye Disease Study Group. Br. J. Ophthalmol. **80:**969–972.
81. **Willey, D. E., M. D. Trousdale, and A. B. Nesburn.** 1984. Reactivation of murine latent HSV infection by epinephrine iontophoresis. Invest. Ophthalmol. Vis. Sci. **25:**945–950.
82. **Yi, J. S., M. Du, and A. J. Zajac.** 2009. A vital role for interleukin-21 in the control of a chronic viral infection. Science **324:**1572–1576.
83. **Zajac, A. J., et al.** 1998. Viral immune evasion due to persistence of activated T cells without effector function. J. Exp. Med. **188:**2205–2213.